Int. J. Nano Dimens., 13 (2): 144-154, Spring 2022

ORIGINAL ARTICLE

Enhancing the photocatalytic activity of TiO_2 nanoparticles using green Carbon quantum dots

Irié Bi Irié Williams [1, 2], Essy Kouadio Fodjo [2, *], Kouyaté Amadou [3], Trokourey Albert [2], Cong Kong [1, 4]

[1] Key Laboratory of East China Sea Fishery Resources Exploitation, Ministry of Agriculture and Rural Affairs, East China Sea Fisheries Research Institute, Chinese Academy of Fishery Sciences, Shanghai 200090, China

[2] Laboratory of Constitution and Reaction of Matter, UFR SSMT, Université Felix Houphouet Boigny, 22 BP 582 Abidjan 22, Cote d'Ivoire

3 Laboratory of Environmental Sciences and Technology, Université Jean Lorougnon Guédé, BP 150 Daloa, Cote d'Ivoire

[4] Shanghai Key Laboratory of Forensic Medicine (Academy of Forensic Science), Shanghai 200063, China

Received 08 August 2021; revised 12 September 2021; accepted 13 September 2021; available online 20 September 2021

Abstract

A simple and green method based on chemical fragmentation of wood charcoal is used to produce carbon quantum dots (CQDs). These CQDs are used to form a nanocomposite with synthesized titanium dioxide nanoparticles (TiO_2/CQDs). The X-ray diffraction (XRD) analysis of this TiO_2/CQDs nanocomposite has revealed that the presence of CQDs in these TiO_2/CQDs does not affect the TiO_2 NPs crystalline structure; while the characterization using scanning electron microscopy (SEM) analysis shows a porous structure of TiO_2 NPs and TiO_2/CQDs resulting from the aggregation of nanoparticles with a mean size of around 25 nm and 30 nm for TiO_2 NPs and TiO_2/CQDs, respectively. Furthermore, a transmission electron microscopy (TEM) analysis displays particle size around 4 nm for CQDs. Besides, the reflectance study in the visible range shows that the presence of CQDs reduces the reflection of sunlight by TiO_2 NPs in TiO_2/CQDs nanocomposite. Moreover, compared to TiO_2 NPs, TiO_2/CQDs have a higher rate for methylene blue (MB) photocatalytic degradation. Indeed, an efficiency of up to 100% within ten minutes of sun exposure for the degradation of 7.5 mg/L MB can be achieved using TiO_2/CQDs in opposition to thirty minutes using TiO_2NPs under the same conditions. This efficiency is obviously due to the reduction of the reflective properties of TiO_2 NPs in the visible range by the presence of CQDs in the TiO_2/CQDs nanocomposite. These results suggest that TiO_2/CQDs could be used as heterogeneous photocatalyst for the degradation of similar compounds in water bodies under solar irradiation.

Keywords: *Carbon Quantum Dots (CQDs); Fluorescent CQDs; Methylene Blue Photocatalytic Degradation; Reduction of TiO_2 Reflective Property; TiO_2 Nanoparticle Synthesis.*

How to cite this article

Williams I.B.I, Kouadio Fodjo E., Amadou K., Albert T., Kong C. Enhancing the photocatalytic activity of TiO_2 nanoparticles using green Carbon quantum dots. Int. J. Nano Dimens., 2022; 13(2): 144-154.

INTRODUCTION

Excessive use of chemicals, especially the high production of synthetic dyes from paper, cosmetics, food and textile industries has contributed to environmental pollution [1, 2]. The annual dye production is estimated to be about seven hundred thousand tons with approximately one hundred thousand types of dyes. Owing to their high consumption in various fields, a large quantity of these dyes is directly released into the water bodies without pretreatment [3]. However, even at low concentrations (< 1 ppm), dyes can seriously reduce the light penetration

* Corresponding Author Email: *kouadio.essy@univ-fhb.edu.ci*

in water environment and affect the process of photosynthesis in aquatic environments, leading therefore to a real threat to the aquatic ecosystem [2, 4]. In addition, dyes in water have toxic effects on human health due to their association with certain diseases such as allergies, tumors, cancer, and heart disease [5]. It is, therefore, of paramount importance to develop robust, cost-effective and efficient, environmentally friendly technologies for the degradation or removal of these dyes before their release into the environment. To meet these goals, several techniques such as chemical [6], physicochemical [7], and biological [8] methods have been used for the treatment of these dyes. In these methods, the application of advanced oxidation processes (AOPs) is one of the most effective processes to be implemented for the mineralization of organic compounds. In particular, Fenton reagents and photocatalytic systems can generate reactive radical species to discolor and degrade the dyes in a short time [9]. Unfortunately, the generated sludge requires post-treatment, thus leading to a high cost for its implementation.

In these past decades, photocatalytic systems based on nanomaterials have been the subject of intensive investigation [10-13]. The dimensional characteristic from 1 nm to 100 nm endows these materials with optical, magnetic, electronic and catalytic properties which cannot be obtained with their bulk counterpart [14]. Among these nanomaterials, semiconductor-based nanoparticles such as titanium dioxide nanoparticles (TiO_2 NPs) have been widely used for the removal of organic pollutants [15]. TiO_2 NPs are well known as one of the most promising photocatalysts for wastewater treatment because of their high capacity to fully oxidize organic pollutants, their high chemical stability and their low toxicity [16]. Nevertheless, due to their large energy bands (3.0, 3.1 and 3.2 eV depending on the type of phase), TiO_2 NPs are only sensitive to energy radiation at least equivalent to ultraviolet (UV) radiation, reducing thus the application of TiO_2 in solar systems for the degradation of organic pollutants. Indeed, the UV spectrum represents only around 5% of the total solar spectrum [17]. In order to overcome this limitation, many attempts such as metallic or non-metallic doping [18] and surface deposition of noble metals [19] were tested. In this purpose, carbon quantum dots (CQDs) are raising great interest. The presence of numerous functional groups such as alcohol, carboxylic and carbonyl groups on their surface endows CQDs with high aqueous solubility and binding capability with other reactive groups for surface passivation and functionalization [20, 21]. Besides, CQDs possess unique properties such as high photon absorption efficiency, high biocompatibility, low toxicity, and excellent reservoir of free electrons and electron transfer properties due to their π-conjugated structure [22, 23]. These fascinating features give CQDs a wide application in various fields such as chemical detection, photocatalysis and electrocatalysis as the delocalized π-conjugated structure can induce rapid photogenerated charges separation and charges transfer. In addition, CQDs can transfer two or more low energy photons to a higher energy photon by sequentially absorbing longer wavelength photons, leading therefore to light emission at a wavelength shorter than the excitation wavelength [24]. Moreover, the light-absorbing capacity of CQDs in nanocomposites facilitates photo transfer phenomena of excited electrons across their interfaces by allowing charge stabilization, separation and formation of long-lived holes at the surface [25, 26]. They are thus promising candidates as dopants in the manufacturing of photocatalysts. Studies on composite systems consisting of TiO_2 NPs and carbon-based materials such as carbon nanotubes, fullerenes, graphenes and CQDs are still under intensive investigation. Several works have used diverse sources such as glucose in hydrothermal process [27], graphite rods in an electrochemical etching (oxidation) [28], γ-butyrolactone dehydration with concentrated sulphuric acid for their synthesis. All of these works have shown the sensibility of CQD/TiO_2 nanocomposite to solar. However, those synthesized techniques using biomass as CQDs source are mainly involved in the chemical detection [29]. In addition, in the work of Wang *et al.* [30], CQDs prepared using citric acid as a carbon source via ammonium hydroxide (NH_4OH) through high-temperature (200 °C) in hydrothermal method have allowed to obtain fluorescent CQDs. Such CQDs are loaded not only with alcohol, carboxylic and carbonyl groups on their surface but also with amine groups.

In this current study, CQDs were synthesized by chemical fragmentation via NH_4OH at relatively low temperature (50 °C) using green and economically abundant wood charcoal as carbon source. These

green CQDs were combined with synthesized TiO_2 NPs to form TiO_2/CQDs nanocomposites. The study of the photocatalytic performance for the methylene blue (MB) degradation has shown that TiO_2/CQDs have higher rate than that of TiO_2 NPs. This difference in the TiO_2/CQDs photocatalytic properties is attributed to the reduction of the reflective properties of TiO_2 NPs by CQDs in TiO_2/CQDs in the visible region. These TiO_2/CQDs nanocomposite can thus serve as a photocatalyst for the degradation of similar structurally organic compounds with considerable efficiency in the water environment under solar irradiation. This ability of CQDs prepared by a green method to improve the photocatalytic properties of TiO_2 NPs by reducing the reflective properties of semiconductors could be an innovative approach to provide efficient photocatalysts.

MATERIALS AND METHODS

Reagents

All chemicals used in this study were of analytical grade and were used as received without any further purification. Titanium isopropoxide ($C_{12}H_{28}O_4Ti$, 97 %) and potassium hydroxide (KOH, 85 %) were purchased from Sigma Aldrich (St. Louis, MO, USA). Methylene blue ($C_{16}H_{18}ClN_3S$, 98 %) was purchased from Merck (Darmstadt, Germany). Ethanol (C_2H_5OH, 98 %), hydrochloric acid (HCl, 37 %) and acetone (C_3H_6O, 98 %) were supplied by Panreac quimica (Barcelona, Spain) and ammonium hydroxide (NH_4OH, 28-30 %) was supplied by Honeywell Fluka (Buchs, Switzerland). Deionized (DI) water used throughout this study was obtained from the water purification system (Sichuan Zhuoyue Water Treatment Equipment Co., Ltd, Chengdu, China). It allows the acquisition of DI water with a resistivity of 18.25 MW•cm. The wood charcoal used to synthesize the CQDs was obtained from the local market (Abidjan, Ivory Coast).

Synthesis of CQDs, TiO_2 NPs and TiO_2/CQDs nanocomposites

The colloidal CQDs were obtained according to the procedure described in the literature [30]. In a typical synthesis procedure, 50 mL of 2.5 M NH_4OH solution was prepared from commercial NH_4OH by dilution in DI water. Then, 500 mg of powdered charcoal was added to this solution (previously brought to 50 °C in a water bath with magnetic stirring at 500 rpm in fume hood for 10 min) followed by gently stirring at 50 °C for 12 h. The obtained solution was then cooled to room temperature and centrifuged at 4000 rpm for 5 min using Tabletop High-Speed centrifuge (MRC Ltd., Holon, Israel) to remove the macro-particles. To the recovered supernatant, DI water was added to reach 25 mL. The newly obtained solution was once again heated at 50 °C in the water bath under stirring at 500 rpm for 10 min. To this solution, 17 mL of 2.5 M NH_4OH solution was added and the solution was filled with DI water to reach a final volume of 50 mL. The resulting solution was kept at 50 °C under gently stirring for another 12 h. The obtained solution was cooled to room temperature and then centrifuged at 4000 rpm for 5 min to finally obtain the colloidal CQDs.

For the synthesis of TiO_2 NPs, the "sol-gel" process at moderate temperature as reported previously with slight modification, was used [31]. Firstly, 40 mL of $Ti[OCH(CH_3)_2]_4$ was mixed with 80 mL of ethanol under stirring (500 rpm) for 10 min at room temperature (28 °C). Then, 80 mL of DI water previously adjusted at pH 9 using 0.1 N KOH was dropwisely added to the solution. The obtained solution was kept under stirring (500 rpm) at room temperature until a white paste was obtained. This paste was then centrifuged and dried in an oven for 12 h at 100 °C and calcined in air at 400 °C for 3 h at a temperature rising rate of 5 °C/min to obtain the TiO_2 NPs.

The nanocomposites consisting of CQDs and TiO_2 NPs (TiO_2/CQDs) were synthesized according to the previously reported procedure [32]. Briefly, 250 mg of previously synthesized TiO_2 NPs were dispersed in 125 mL of ethanol under vortex agitation for 10 min. To this solution, 50 µL of the obtained colloidal solution of CQDs was added. This mixture was stirred at 500 rpm for 30 min at room temperature. The obtained solution was collected by centrifugation, washed three times with ethanol and oven dried at 100 °C for 3 h to finally obtain the TiO_2/CQDs nanocomposites.

Characterization of the synthesized nanostructures

The X-ray diffraction (XRD) characterization of the different samples was performed using a diffractometer type Siemens D5005 (Simens AG, Munich, Germany) with a copper anticathode ($\lambda_{K\alpha1}$=1.5406 Å). The angle of incidence (2Θ) varies from 5 to 90 °C. Moreover, the absorbance and the reflectance were measured using UV-Vis spectrometer Flame-S-XR1 (Ocean Optics,

Largo, USA) while the fluorescence of CQDs was investigated with Qiwei WFH-204B portable UV lamp 254/365 nm (Hangzhou, China). However, the morphological characterization of TiO_2 NPs and TiO_2/CQDs was performed by scanning electron microscopy (SEM) with JSM-6010LA apparatus (JEOL Ltd., Tokyo, Japan) and CQDs were characterized by transmission electron microscopy (TEM) using a JEOL JEM-2010 apparatus (Tokyo, Japan).

Photocatalytic analysis

Determination of the degradation percentage of MB

In order to take a maximum advantage of the solar irradiation, all photocatalytic experiments were carried out between 11:00 AM and 3:00 PM and when there were no clouds in the sky. To analyze the photocatalytic properties of TiO_2 and TiO_2/CQDs nanostructures, 250 mg of TiO_2 NPs (or TiO_2/CQDs) was added in a beaker containing 100 mL of 7.5 mg/L MB chosen as a model. After 30 min of shaking in the dark to reach the adsorption-desorption equilibrium [33], the mixture is irradiated with sunlight at different times (30, 60, 90, 120, 150, 180 min for TiO_2 NPs and 10, 20, 30, 40, 50 min for TiO_2/CQDs). Under supervision, samples were taken every 30 min and 10 min for TiO_2 NPs and TiO_2/CQDs, respectively, for measurement after collection of the suspension by centrifugation. The concentration of residual MB in the centrifuged solution was analyzed by measuring the absorbance at 664 nm (characteristic peak of MB). The degradation percentage of the dye in the presence of TiO_2 NPs or TiO_2/CQDs was then estimated using Equation (1):

$$\%D = \frac{C_0 - C_t}{C_0} \times 100 \quad (1)$$

where C_0 represents the initial MB dye concentration and C_t represents its concentration after solar irradiation at a time t.

Influence of the initial MB concentration on its degradation

A series of experiments was conducted to study the effect of initial concentration of MB by varying its concentration (5 mg/L, 7.5 mg/L, 10 mg/L, 12.5 mg/L and 15 mg/L). For this purpose, in 100 mL of each solution, 250 mg of TiO_2 NPs (or TiO_2/CQDs) was added. The resulting mixture was kept in the dark under stirring at 500 rpm for 30 min to reach the adsorption-desorption equilibrium. Once equilibrium is reached, the five beakers containing the different concentrations of MB were exposed to natural sunlight. Samples of 2 mL were taken every 30 min and centrifuged at 4000 rpm for 5 min. The collected supernatant was measured with the UV-Vis spectrophotometer to evaluate the residual MB.

Influence of the catalyst mass on the MB degradation and kinetic study of MB degradation

The influence of the mass of TiO_2 NPs for their ability to act as a photocatalyst for the degradation of MB was evaluated. In detail, 100 mg, 150 mg, 200 mg, 250 mg, 300 mg, and 350 mg of TiO_2 NPs were examined in 100 mL of 7.5 mg/L MB. After the adsorption-desorption equilibrium, the six beakers containing these different solutions were exposed to sunlight. Subsequently, 2 mL of the samples was taken every 30 min and centrifuged at 4000 rpm and then the residual MB was evaluated.

The study of the photocatalytic reaction kinetics of the MB was performed using initial MB concentrations of 5 mg/L, 7.5 mg/L, 10 mg/L, 12.5 mg/L, and 15 mg/L in a solution containing 250 mg of TiO_2 NPs. More Information can be found in Supplemental Materials.

Influence of pH on the MB degradation

To assess the effect of pH on the synthesized TiO_2/CQDs and TiO_2 NPs photocatalytic activity, a series of experiments was carried out, varying the pH of the solution from 2 to 13 (pH 2, 4, 7, 9, 11 and 13). The solution was adjusted using 0.1 N HCl or 0.1 N KOH. For each given pH, 250 mg of TiO_2/CQDs or TiO_2 NPs was dispersed in 100 mL of 7.5 mg/L MB. After reaching the adsorption-desorption equilibrium, the six different solutions were exposed to sunlight for 2 h in the case of TiO_2 NPs and 40 min for TiO_2/CQDs nanocomposite. Two milliliters of each solution were taken every 15 min for TiO_2 NPs and 5 min for TiO_2/CQDs, and centrifuged at 4000 rpm. The collected supernatant was measured with the UV-Vis spectrometer to evaluate the residual MB.

RESULTS AND DISCUSSION

Characterization of the synthesized nanostructures

In order to know the features of the synthesized materials, the characterization with SEM and TEM

of the different samples, as well as the absorbance of CQDs and the reflectance of TiO_2/CQDs were performed. Fig. 1a shows the TEM image of the synthesized materials from wood charcoal. In this figure, spherical and uniformly dispersed particles with a mean size of about 4 nm are observed, clearly indicating that carbon dots are obtained by the synthesis method. This assertion is confirmed by the absorption spectrum (Fig. 1b), which exhibits a characteristic intense peak of CQDs around 226 nm with a shoulder around 270 nm. Indeed, the peak observed around 226 nm is attributed to the π-π* transition of the C=C bonds, while the shoulder around 270 nm is associated with n-π* transition of the C-O or C-N bonds, suggesting the synthesis of CQDs with terminals rich in carboxylic, carbonyl, amine and alcohol functional groups [30, 34]. In addition, under irradiation with 365 nm wavelength of a UV lamp, these particles display green light (Inset of Fig. 1b), which may be the result of n-π* electronic transitions, thus corroborating that the synthesized materials are CQDs [25].

Besides, the morphology of TiO_2 NPs and TiO_2/CQDs was evaluated with SEM (Fig. 1c & Fig. 1d, respectively). The results show that these substrates are in nanoscale size with spherical forms. In general, porous structures from the aggregation of nanoparticles with size about 30 nm and 25 nm of TiO_2 NPs and TiO_2/CQDs are obtained, respectively. These nanostructures lead to a sponge-like structure, especially in the case of TiO_2/CQDs in which the pores are larger than those of TiO_2 NPs. These resultants suggest

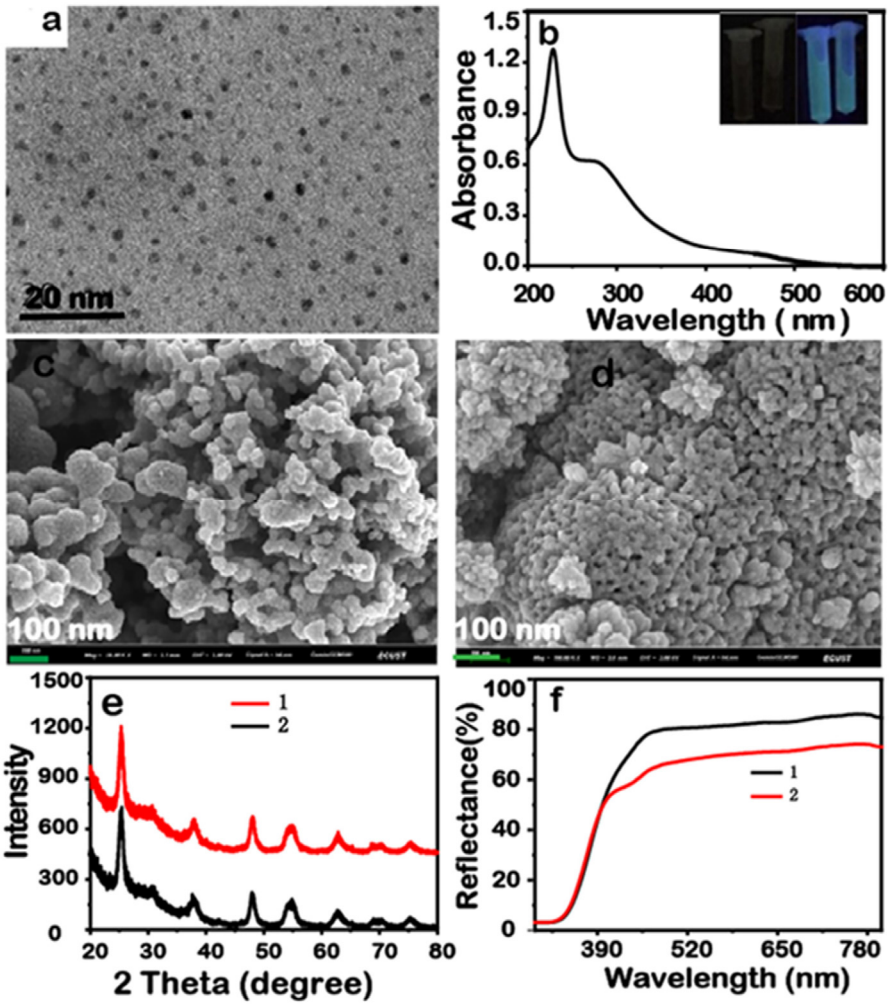

Fig. 1. a) TEM image and b) absorption spectrum of CQDs (inset, fluorescence image of CQDs under sunlight and 365 nm UV lamp), SEM images of c) TiO_2 NPs and d) TiO_2/CQDs. e) XRD spectra and f) reflectance spectra of TiO_2 NPs (1) and TiO_2/CQDs (2).

that the addition of CQDs helps to increase the porosity and the aggregation effect of TiO_2 NPs in TiO_2/CQDs. These different forms could play an important role in photocatalytic application.

Moreover, in order to know the crystal structure of the synthesized particles, the TiO_2 NPs and TiO_2/CQDs were characterized by XRD (Fig. 1e). The obtained diffraction patterns were compared with the data sheet (JCPDS card No. 028-1192). Both TiO_2 NPs and TiO_2/CQDs nanocomposite display obvious peaks at 2θ of 25.5°, 37.3°, 48.15°, 53.94°, 55.14°, 62.88°, 68.86°, 70.36°, and 75.18° which can be assigned to the (101), (103), (200), (105), (211), (204), (116), (220), and (215) of the anatase TiO_2, respectively. This result is in good agreement with the standard JCPDS data sheet and the literature [27]. The obtained TiO_2/CQDs and TiO_2 NPs have similar profiles and typical spectrum of anatase structure. In addition, no diffraction peak shifts or peak intensity changes in TiO_2/CQDs peaks with respect to those of TiO_2 NPs are observed, suggesting that the crystalline phase of TiO_2 NPs is not affected by the presence of CQDs in the TiO_2/CQDs nanocomposite [35]. These results indicate that CQDs are well deposited on the TiO_2 surface and not incorporated into the TiO_2 crystal lattice [23]. This result may confirm the growth in size of the TiO_2/CQDs particles compared to those of TiO_2 NPs in the SEM images.

Furthermore, to demonstrate the effect of the synthesized CQDs in the TiO_2/CQDs nanocomposites, the reflectances of TiO_2 NPs and TiO_2/CQDs were investigated in the UV-Vis range. As displayed in Fig. 1f, the reflectance of TiO_2 NPs is higher than that of the TiO_2/CQDs nanocomposite in the visible range. This low reflective property of TiO_2/CQDs suggests that the coupling of TiO_2 NPs with CQDs leads to a significant reduction of the reflection of light rays by the TiO_2 NPs in the visible region. This decrease in reflectance of this nanocomposite compared to that of TiO_2 NPs may be attributed to chemical bonds between TiO_2 and CQDs [36]. This decrease in reflective activity of TiO_2/CQDs suggests that the photocatalytic activity of TiO_2/CQDs may be better than that of TiO_2 under visible light irradiation [23].

Photocatalytic properties of synthesized nanostructures

Degradation of MB using the synthesized nanostructures as catalyst under solar irradiation

In order to study the photocatalytic properties of the synthesized TiO_2 NPs and TiO_2/CQDs, the degradation of MB in an aqueous medium was examined (Fig. 2a). In this figure, it can be observed that the characteristic peak of MB in the presence of TiO_2 NPs decreases rapidly during the first 30 min of irradiation. Beyond 120 min of irradiation

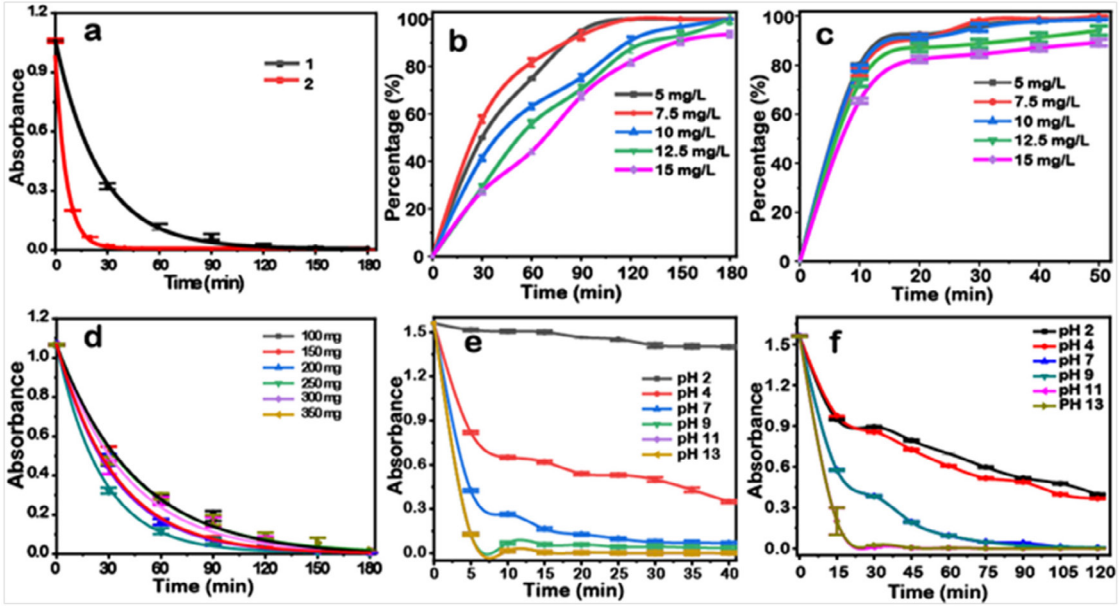

Fig. 2. a) Degradation of 7.5 mg/L MB under sun exposure using TiO_2 NPs (1) and TiO_2/CQDs (2). Removed percentage of MB at different times with b) TiO_2 NPs and c) TiO_2/CQDs. d) MB (7.5 mg/L) degradation for different masses of TiO_2NPs at different times. Effect of pH with e) TiO_2 NPs and f) TiO_2/CQDs on the degradation of 7.5 mg/L MB.

(Fig. S1a and Fig. S1b), the peak is not noticeable while in the presence of TiO_2/CQDs, the same peak undergoes fast decrease within 10 min and totally disappears within 30 min. This disappearance of the peak indicates the complete degradation of MB by TiO_2 NPs or TiO_2/CQDs, suggesting that this TiO_2 NPs and TiO_2/CQDs are excellent photocatalysts agents for the degradation of MB in water environment [37]. However, TiO_2/CQDs are the best photocatalysts as their associated time for the MB degradation is shorter than that of TiO_2 NPs.

Influence of the initial MB concentration on the degradation rate of MB

To further demonstrate the influence of the initial concentration of MB on the rate of its degradation process, different initial concentrations of MB were assessed (Fig. 2b, 2c). The results in both cases (TiO_2 NPs and TiO_2/CQDs) show that the rate of degradation of MB decreases with the increase in the initial MB concentration. This decrease effect can be attributed to the formation of several layers of the adsorbed MB on the surface of TiO_2 NPs and TiO_2/CQDs for a high concentration of the dye, which make the TiO_2 NPs and TiO_2/CQDs sites inaccessible to the photons [38]. For higher MB concentration, the generation of $^{\bullet}OH$ radicals on the surface of the photocatalysts is therefore reduced after adsorption of these layers. A significant amount of sunlight is thus absorbed by the dye molecules themselves, shielding the hotspot on the photocatalysts.

Influence of the mass of TiO_2 NPs on the rate of MB degradation

In order to determine the optimal mass of TiO_2 NPs in the photocatalytic degradation of MB, experiments were performed in the presence of sunlight with different masses of TiO_2 NPs (Fig. 2d). As displayed, in general, the addition of TiO_2 NPs in the solution promptly leads to the removal of a large amount of MB in the first thirty minutes of irradiation, especially for a mass less than 250 mg of TiO_2 NPs (with an optimum effect at 250 mg), where it is even possible to completely remove MB after 120 min of solar irradiation. However, for a mass higher than 250 mg, although there is a significant degradation, total degradation seems to be possible over a long period of solar irradiation. The presumed reason could be due to the turbidity of the solution, which increases with the increase of TiO_2 mass, reducing therefore the efficiency of the catalytic reaction [39]. The rapid and total photocatalytic degradation of MB after 120 min using 250 mg of TiO_2 NPs, suggests that this mass corresponds to the optimal mass of TiO_2 NPs for which a maximum exposed surface is fully illuminated and a large number of photogenerated active species ($^{\bullet}OH$ and h^+) is produced in the medium, so this mass is used for the following experiments. This result is in good agreement with the literature [40, 41]. Indeed, no improvement in the rate of degradation is necessary with the increasing amount of TiO_2 NPs above a certain value. This complete degradation of MB by TiO_2 NPs under sunlight irradiation suggests that TiO_2 NPs is an excellent photocatalyst for the degradation of MB in water environment.

Influence of the pH on the rate of MB degradation

To study the pH effect on the efficiency of MB degradation using TiO_2 NPs and TiO_2/CQDs as photocatalysts, different pH were evaluated (Figs. 2e and 2f). From these figures, it can be observed that the rate of MB degradation increases with increasing pH in both cases. The best degradation (100%) is obtained with a pH 11 and beyond within 30 min and 10 min for TiO_2 NPs and TiO_2/CQDs, respectively. As MB is cationic, it is obvious that its adsorption on the photocatalyst surface is less important in acidic media due to the repulsive forces between the positive catalyst surface and the MB molecules. However, in alkaline media, there is an attractive electrostatic interaction between the negative catalyst surface and the positive charge of the MB molecules, leading to an adsorption of MB on the catalyst surface. In addition, the presence of a large amount of OH^- ions on the surface of the catalyst as well as in the reaction medium promotes the formation of $^{\bullet}OH$ radicals, which are widely known to be the main oxidizing species responsible for the MB degradation [37]. Furthermore, in the case of CQDs, the alkaline solution may also promote carboxylate ions and the availability of amine function which may play an additional role in CQDs efficiency effect. Therefore, pH 11 is selected for the rest of the experiments.

Kinetics of MB degradation

In a photocatalytic study, the elaboration of kinetics associated with the reaction mechanism is based on the influence of the initial

concentration of the substrate on the rate of the reaction progress. Therefore, the study of the photocatalytic reaction kinetics of MB was carried out. The photodegradation kinetic constants of MB were determined using Equations (S1) and (S2) for pseudo-first (Fig. S2a and Fig. S2b) and pseudo-second order (Fig. S2c and Fig. S2d) for TiO_2 NPs and TiO_2/CQDs, respectively. The velocity constants k_1, and the different correlation coefficients R^2 of MB are given in Table 1. The results give R^2 values closer to 1 for pseudo-first-order compared with those of pseudo-second-order where R^2 is relatively far to 1 in both cases, suggesting that the photocatalytic degradation of MB follows apparent first-order kinetics. Moreover, it should be noted that k_1 decreases with an increase in MB concentration. This decrease is consistent with the MB shielding effect previously described. In addition, the k_1 values for TiO_2/CQDs are 4 to 10 folds higher than those obtained with TiO_2 NPs, confirming the excellent photocatalytic properties of TiO_2/CQDs.

To better describe the phenomenon, the study of MB adsorption isotherms on TiO_2 NPs and TiO_2/CQDs was also performed using Langmuir-Hinshelwood and Temkin isotherms which are widely used in photocatalytic studies (Fig. S2e-h). As summarized in Table 2, the Langmuir-Hinshelwood kinetic model displays the best agreement for the degradation kinetics of MB (higher R^2 and closer to 1), suggesting that the chemical transformation of MB takes place on the surface of the photocatalysts. Indeed, at least one of the steps of the reaction mechanism involves the adsorption of more reactants, and the adsorbed molecules undergo a bimolecular reaction at neighboring sites. This result is in good agreement with the literature in which the Langmuir-Hinshelwood model is widely used to describe the experimental results in heterogeneous photocatalysis [42, 43]. However, Temkin kinetic model can also be considered as its correlation coefficient is also relatively close to one (R^2 = 0.9). This behavior can explain the low degradation efficiency when the MB concentration increases. In fact, Temkin isotherm model assumes that the adsorption heat of all molecules decreases linearly with the increase in coverage of the adsorbent surface. Therefore, it can be accepted that the MB degradation follows both Langmuir-Hinshelwood and Temkin model on TiO_2 NPs and TiO_2/CQDs.

Application

In order to study the applicability of the synthesized TiO_2 NPs and TiO_2/CQDs photocatalysts in real samples, wastewater from the University Hospital Center of Cocody (UHCC) was examined. The spectrum of this UHCC wastewater indicates a wide band between 200-400 nm (Fig. S5a and Fig. S5b). The evolution over time of this peak, in the presence of the photocatalysts (TiO_2 NPs or TiO_2/CQDs), shows that only the shoulder of this wide band disappears, suggesting that the UHCC wastewater may contain non-degradable pollutants by TiO_2 NPs and TiO_2/CQDs such as ions as indicated by its conductivity. Moreover, discoloration of this wastewater occurs within 50 min and 30 min for TiO_2 NPs and TiO_2/CQDs, respectively (Fig. S5a and Fig. S5b), indicating that these photocatalysts can be used for this

Table 1. Kinetics parameters of MB degradation.

Initial Concentration du MB (mg/L)	Pseudo-first order				Pseudo-second order	
	k_1 (min^{-1})		R^2		R^2	
	TiO_2 NPs	TiO_2/CQDs	TiO_2 NPs	TiO_2/CQDs	TiO_2 NPs	TiO_2/CQDs
5	0.0255	0.1053	0.9969	0.9777	0.8671	0.6716
7.5	0.01395	0.1298	0.9888	0.9995	0.8669	0.8548
10	0.01683	0.1443	0.9863	0.9659	0.8808	0.4185
12.5	0.01494	0.1169	0.9700	0.9772	0.8943	0.8184
15	0.0153	0.0888	0.95833	0.9483	0.96615	0.7006

Table 2. Equilibrium parameters of the MB adsorption isotherms on TiO_2 NPs and TiO_2/CQDs.

Models	R^2		k_{L-H}		Ln k_t		B_1	
	a*	b*	a*	b*	a*	b*	a*	b*
Langmuir-Hinshewood	0.986	0.988	0.0168	0.1298	…….	……	…….	……
Temkin	0.901	0.966	……	……..	-2.875	-12.624	-0.887	-0.208

*a: TiO_2 NPs and b: TiO_2/CQDs

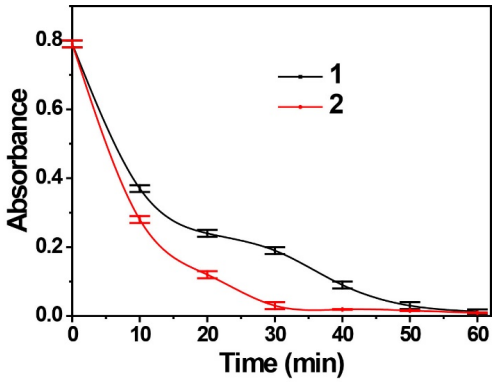

Fig. 3. UHCC Water degradation after adding 7.5 mg/L MB, using TiO_2 NPs (1) and TiO_2/CQDs (2) as photocatalyst.

wastewater discoloration. Furthermore, the characteristic peak at 664 nm of MB in the UHCC wastewater contaminated with MB was studied in the presence of 250 mg of TiO_2 NPs or TiO_2/CQDs under irradiation of sunlight at room temperature (Fig. 3). As displayed, the peak at 664 nm decreases quickly for the first ten minutes of sun exposure in both cases. However, a fast MB degradation is noted in the case of TiO_2/CQDs, confirming that TiO_2/CQDs are more efficient than TiO_2 NPs for the MB degradation in wastewater. This discoloration of the UHCC wastewater and degradation of an organic pollutant in wastewater in the presence of TiO_2 NPs or TiO_2/CQDs suggest that these nanostructures may be efficient photocatalysts for water bodies. Furthermore, the time required for the degradation of MB in the wastewater is slightly higher than that obtained in DI water for TiO_2/CQDs. This difference is probably due to the possible competitive effect of the presence of additional compounds affecting the CQDs, as indicated by the absorbance peak around 245 nm (Fig. S1) and the conductivity of UHCC wastewater [44].

CONCLUSION

In this work, TiO_2 NPs and TiO_2/CQDs nanocomposites are synthesized. In particular, CQDs are synthesized using wood charcoal as carbon source. The study of their photocatalytic properties shows that the MB degradation follows apparent first-order kinetics, and both Langmuir-Hinshelwood and Temkin model describes the MB degradation kinetics, indicating that the chemical transformation of MB takes place at the surface of the photocatalysts. Besides, TiO_2/CQDs have exhibited the best photocatalytic degradation rate compared to TiO_2 NPs and, its efficiency can reach 100 % within 10 min, whereas it may take 30 min with TiO_2 NPs for the total degradation of MB under sun exposure. This efficiency seems to be due to the reduction of the reflective properties of TiO_2 NPs in the visible range by the synthesized CQDs in TiO_2/CQDs nanocomposites. TiO_2/CQDs could therefore be used as a photocatalyst for the degradation of organic compounds in the water environment under solar irradiation.

ACKNOWLEDGMENTS

The authors would like to thank the financial support from the National Natural Science Foundation of China (31701698) and Shanghai Key Laboratory of Forensic Medicine (Academy of Forensic Science, KF1910).

DECLARATION OF INTERESTS

The authors declare that they have no known competing financial interests or personal relationships that could have appeared to influence the work reported in this paper

REFERENCES

[1] Padhi B. S., (2012), Pollution due to synthetic dyes toxicity & carcinogenicity studies and remediation. *Int. J. Environ. Sci.* 3: 940-955.

[2] Pereira L., Alves M., (2012), Dyes—environmental impact and remediation. *In Environmental Protection Strategies for Sustainable Development*. (pp. 111-162): Springer.

[3] Martínez-Huitle C. A., Brillas E., (2009), Decontamination of wastewaters containing synthetic organic dyes by electrochemical methods: A general review. *Appl. Catal. B-Environ.* 87: 105-145.

[4] Gita S., Hussan A., Choudhury T., (2017), Impact of textile dyes waste on aquatic environments and its treatment. *Environ. Ecol.* 35: 2349-2353.

[5] Lovato M. E., Fiasconaro M. L., Martín C. A., (2017), Degradation and toxicity depletion of RB19 anthraquinone dye in water by ozone-based technologies. *Water Sci. Technol.* 75: 813-822.

[6] Xu C., Zhang B., Wang Y., Shao Q., Zhou W., Fan D., Bandstra J. Z., Shi Z., Tratnyek P. G., (2016), Effects of sulfidation, magnetization, and oxygenation on azo dye reduction by zerovalent iron. *Environ. Sci. Technol.* 50: 11879-11887.

[7] Sansuk S., Srijaranai S., Srijaranai S., (2016), A new approach for removing anionic organic dyes from wastewater based on electrostatically driven assembly. *Environ. Sci. Technol.* 50: 6477-6484.

[8] Khan R., Bhawana P., Fulekar M. H., (2013), Microbial decolorization and degradation of synthetic dyes: A review. *Rev. Environ. Sci. Biotechnol.* 12: 75-97.

[9] Salgado P., Melin V., Durán Y., Mansilla H. C., Contreras D., (2017), The reactivity and reaction pathway of Fenton reactions driven by substituted 1, 2-dihydroxybenzenes. *Environ. Sci. Technol.* 51: 3687-3693.

[10] Nair Sreekala G., Abdullakutty F., Beena B., (2019), Green synthesis, characterization, and photo catalytic degradation efficiency of Trimanganese Tetroxide nanoparticle. *Int. J. Nano Dimens.* 10: 400-409.

[11] Golshan Tafti A., Rashidi A., Tayebi H.-A., Yazdanshenas M. E., (2018), Comparison of different kinetic models for adsorption of acid blue 62 as an environmental pollutant from aqueous solution onto mesoporous Silicate SBA-15 modified by Tannic acid. *Int. J. Nano Dimens.* 9: 79-88.

[12] Fekri M. H., Bazvand R., Soleymani M., Razavi Mehr M., (2020), Adsorption of Metronidazole drug on the surface of nano fullerene C60 doped with Si, B and Al: A DFT study. *Int. J. Nano Dimens.* 11: 346-354.

[13] Azari B., Pourahmad A., Sadeghi B., Mokhtary M., (2019), Preparation and photocatalytic study of SiO_2/CuS coreshell nanomaterial for degradation of methylene blue dye. *Nanoscale*. 6: 103-114.

[14] Hong N. H., (2019), Introduction to nanomaterials: basic properties, synthesis, and characterization. In *Nano-Sized Multifunctional Materials*. (pp. 1-19). Seoul National University, South Korea: Elsevier.

[15] Kumar S. G., Devi L. G., (2011), Review on modified TiO_2 photocatalysis under UV/Visible light: Selected results and related mechanisms on interfacial charge carrier transfer dynamics. *J. Phys. Chem. A*. 115: 13211-13241.

[16] Hu X., Hu X., Tang C., Wen S., Wu X., Long J., Yang X., Wang H., Zhou L., (2017), Mechanisms underlying degradation pathways of microcystin-LR with doped TiO_2 photocatalysis. *Chem. Eng. J.* 330: 355-371.

[17] Chen X., Liu L., Huang F., (2015), Black titanium dioxide (TiO_2) nanomaterials. *Chem. Soc. Rev.* 44: 1861-1885.

[18] Ioannidou E., Frontistis Z., Antonopoulou M., Venieri D., Konstantinou I., Kondarides D. I., Mantzavinos D., (2017), Solar photocatalytic degradation of sulfamethoxazole over tungsten–modified TiO_2. *Chem. Eng. J.* 318: 143-152.

[19] Espino-Estévez M., Fernández-Rodríguez C., González-Díaz O. M., Araña J., Espinós J., Ortega-Méndez J. A., Doña-Rodríguez J. M., (2016), Effect of TiO_2–Pd and TiO_2–Ag on the photocatalytic oxidation of diclofenac, isoproturon and phenol. *Chem. Eng. Sci.* 298: 82-95.

[20] Lim S. Y., Shen W., Gao Z., (2015), Carbon quantum dots and their applications. *Chem. Soc. Rev.* 44: 362-381.

[21] Kushwaha N., Mittal J., Pandey S., Kumar R., (2018), High temperature acidic oxidation of multiwalled Carbon nanotubes and synthesis of Graphene quantum dots. *Int. J. Nano Dimens.* 9: 191-197.

[22] Ding H., Yu S.-B., Wei J.-S., Xiong H.-M., (2016), Full-color light-emitting carbon dots with a surface-state-controlled luminescence mechanism. *ACS Nano*. 10: 484-491.

[23] Kumar M. S., Yasoda K. Y., Kumaresan D., Kothurkar N. K., Batabyal S. K., (2018), TiO_2-carbon quantum dots (CQD) nanohybrid: Enhanced photocatalytic activity. *Mater. Res. Express*. 5: 075502.

[24] Shen J., Zhu Y., Yang X., Li C., (2012), Graphene quantum dots: emergent nanolights for bioimaging, sensors, catalysis and photovoltaic devices. *Chem. Commun.* 48: 3686-3699.

[25] Zhang Y., Yuan R., He M., Hu G., Jiang J., Xu T., Zhou L., Chen W., Xiang W., Liang X., (2017), Multicolour nitrogen-doped carbon dots: Tunable photoluminescence and sandwich fluorescent glass-based light-emitting diodes. *Nanoscale*. 9: 17849-17858.

[26] Guo Y., Zhang J., Zhou D., Dong S., (2018), Fabrication of Ag/CDots/BiOBr ternary photocatalyst with enhanced visible-light driven photocatalytic activity for 4-chlorophenol degradation. *J. Mol. Liq.* 262: 194-203.

[27] Zhang X., Wei W., Zhang S., Wen B., Su Z., (2019), Advanced 3D nanohybrid foam based on graphene oxide: Facile fabrication strategy, interfacial synergetic mechanism, and excellent photocatalytic performance. *Science China Mater.* 62: 1888-1897.

[28] Rani S., Borse P. H., Pareek A., Rajalakshmi N., Dhathathreyan K. S., (2016), Photo-Current enhancement in carbon quantum dots functionalized Titania nanotube arrays. *J. Nanosc. Nanotechnol.* 16: 5999-6004.

[29] Thangaraj B., Solomon P. R., Ranganathan S., (2019), Synthesis of Carbon quantum dots with special reference to biomass as a source: A Review. *Current Pharmac. Design*. 25: 1455-1476.

[30] Wang S., Zhu Z., Chang Y., Wang H., Yuan N., Li G., Yu D., Jiang Y., (2016), Ammonium hydroxide modulated synthesis of high-quality fluorescent carbon dots for white LEDs with excellent color rendering properties. *Nanotechnol.* 27: 295202-295206.

[31] Marchal C., Behr M., Vigneron F., Caps V., Keller V., (2016), Au/TiO_2 photocatalysts prepared by solid grinding for artificial solar-light water splitting. *New J. Chem.* 40: 4428-4435.

[32] Muthulingam S., Bae K. B., Khan R., Lee I.-H., Uthirakumar P., (2016), Carbon quantum dots decorated N-doped ZnO: Synthesis and enhanced photocatalytic activity on UV, visible and daylight sources with suppressed photocorrosion. *J. Environ. Chem. Eng.* 4: 1148-1155.

[33] Sun W., Meng S., Zhang S., Zheng X., Ye X., Fu X., Chen S., (2018), Insight into the transfer mechanisms of photogenerated carriers for heterojunction photocatalysts with the analogous positions of valence band and conduction band: A case study of ZnO/TiO_2. *J. Phys. Chem. C*. 122: 15409-15420.

[34] Lin L., Zhang S., (2012), Creating high yield water soluble luminescent graphene quantum dots via exfoliating and disintegrating carbon nanotubes and graphite flakes. *Chem. Commun.* 48: 10177-10179.

[35] Kim D. S., Kwak S.-Y., (2007), The hydrothermal synthesis of mesoporous TiO_2 with high crystallinity, thermal stability, large surface area, and enhanced photocatalytic activity. *Appl. Catal. A: Gen.* 323: 110-118.

[36] Martins N. C., Ângelo J., Girão A. V., Trindade T., Andrade L., Mendes A., (2016), N-doped carbon quantum dots/TiO_2 composite with improved photocatalytic activity. *Appl. Catal. B-Environ.* 193: 67-74.

[37] Yu X., Liu J., Yu Y., Zuo S., Li B., (2014), Preparation and

visible light photocatalytic activity of carbon quantum dots/TiO_2 nanosheet composites. *Carbon*. 68: 718-724.

[38] Khataee A., Sheydaei M., Hassani A., Taseidifar M., Karaca S., (2015), Sonocatalytic removal of an organic dye using TiO_2/Montmorillonite nanocomposite. *Ultrason. Sonochem.* 22: 404-411.

[39] Daneshvar N., Salari D., Khataee A., (2003), Photocatalytic degradation of azo dye acid red 14 in water: Investigation of the effect of operational parameters. *J. Photochem. Photobiol. A Chem.* 157: 111-116.

[40] Silva C. G., Wang W., Faria J. L., (2006), Photocatalytic and photochemical degradation of mono- di-and tri-azo dyes in aqueous solution under UV irradiation. *J. Photochem. Photobiol. A: Chem.* 181: 314-324.

[41] Gupta H., Tanaka S., (1995), Photocatalytic mineralisation of perchloroethylene using titanium dioxide. *Water Sci. Technol.* 31: 47-54.

[42] Ateia M., Alalm M. G., Awfa D., Johnson M. S., Yoshimura C., (2020), Modeling the degradation and disinfection of water pollutants by photocatalysts and composites: A critical review. *Sci. Total Environ.* 698: 134197-134202.

[43] Garcia B. B., Lourinho G., Romano P., Brito P., (2020), Photocatalytic degradation of swine wastewater on aqueous TiO_2 suspensions: Optimization and modeling via Box-Behnken design. *Heliyon*. 6: e03293-e03297.

[44] Atchudan R., Edison T. N. J. I., Perumal S., Karthikeyan D., Lee Y. R., (2017), Effective photocatalytic degradation of anthropogenic dyes using graphene oxide grafting titanium dioxide nanoparticles under UV-light irradiation *J. Photochem. Photobiol. A: Chem.* 333: 92-104.